scientific data

Check for updates

OPEN

DATA DESCRIPTOR

A transcriptome data set for comparing skin, muscle and dorsal root ganglion between acute and chronic postsurgical pain rats

Xiao-yan Meng[1,4], Lan Bu[2,4], Ling Shen[3,4] & Kun-ming Tao[3] ✉

Chronic postsurgical pain (CPSP), with a high prevalence and rising epidemic of opioids crisis, is typically derived from acute postoperative pain. Our knowledge on the forming of chronic pain mostly derives from mechanistic studies of pain processing in the brain and spinal cord circuits, yet most pharmacological interventions targeting CNS came to be unhelpful in preventing CPSP. Revealing the peripheral mechanisms behind the transition from acute to chronic pain after surgery could shine a light on the novel analgesic regimens. Based on two recognized animal models in simulation of acute and chronic postsurgical pain, we provide a next-generation RNA sequencing (RNA-seq) data set to evaluate the time-course transcriptomic variation in the tissue of skin, muscle and dorsal root ganglion (DRG) in these two pain models. The aim of this study is to identify the potential origin and mechanism of the persistent postoperative pain, and further to explore effective and safer analgesic regimens for surgical patients.

Background

Acute pain is ubiquitous in surgical patients, however, some of them may last for a long time and transitions to chronic pain. Chronic postsurgical pain (CPSP), which has been associated with a rising epidemic of opioid abuse and even overdose-related death, is now attaching global attention[1]. The 11th revision of the Internation Classification of Disease defines Chronic postsurgical pain (CPSP) as pain occurs or develops in the incision areas, persists beyond the tissue healing process, and cannot be explained by other causes such as infection or tumor recurrence[2]. The reported prevalence of CPSP varies from 6% to 40% in adults underwent all types of surgeries, while the overall number is prodigious[3–5]. Yet CPSP has been increasingly recognized as a world-wide health problem, as it not only induced discomfort and disability, but also contribute to mal-prescription of opioids. However, clinical understanding on reasons or interventions for CPSP is poor, and the molecular mechanism behind the transition from acute to chronic pain remains elusive[6].

Animal studies in chronic pain has achieved substantial progress in recent years, both peripheral tissue damage and modification in the brain and spinal cord have been proved to play a role in the development of chronic pain[7]. In the central nerve system (CNS), the nociceptive signals are transmitted via ascending projection neurons from spinal cord to cortex, while the noxious signals are also modulated in each level, forming a complicate descending analgesic pathway[8,9]. However, although complete reviews of neurol pathways of pain are available, precise clinical interventions to them is difficult, and outcomes are somehow disappointing. Comparatively, peripheral interventions, such as local anesthetic technics, have achieved more promising outcomes in at least controlling CPSP, if not preventing it[10,11]. Meanwhile, the peripheral tissue damage and somatosensory nerve injury are definitely involved in the initiation and development of chronic pain[12]. Thus, studies focusing on unravel the process of peripheral-neural interaction in the shape of pain after tissue damage is necessary. Previous animal studies already provide us with available animal model for understanding

[1]Department of Critical Care Medicine, Shanghai Eastern Hepatobiliary Surgery Hospital, Naval Medical University, Shanghai, 200438, China. [2]Department of Anesthesiology and Pain Center, Shanghai Changhai Hospital, Navel Medical University, Shanghai, China. [3]Department of Anesthesiology, Shanghai Eastern Hepatobiliary Surgery Hospital, Naval Medical University, Shanghai, 200438, China. [4]These authors contributed equally: Xiao-yan Meng, Lan Bu, Ling Shen. ✉e-mail: kunmingtao@yeah.net; exbh2156@163.com

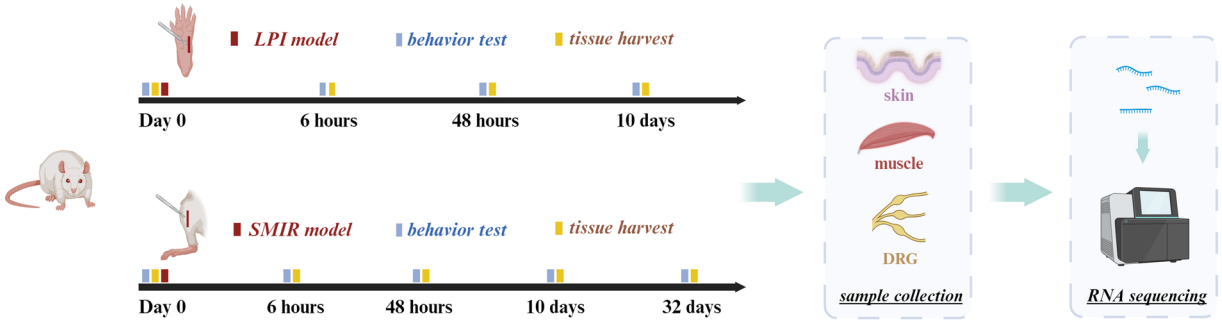

Fig. 1 Experimental workflow. The Skin/Muscle Incision and Retraction (SMIR) and Lateral Paw Incision (LPI) animal models were established, and timepoints for behavior test and the followed tissue harvest as described (N = 4 in each timepoint). Following transcardial perfusion, tissues of the skin, muscle and dorsal root ganglion were extracted, stored and processed for RNA extraction and sequencing.

iatrogenic chronic pain. The Lateral Paw Incision (LPI) model, used a 1 cm incision through the skin to muscle of the rat plantar hindpaw, which could result in a short-term incisional pain which last 48-hours or more in rats, while the Skin/Muscle Incision and Retraction (SMIR) model develops a persistent pain by skin-muscle incision and retraction in the thigh of the rat. These two models are ideal paradigms for understanding postoperative acute and chronic pain, as all of them involved skill-muscle injury and cause reliable nociceptive behaviors under hindpaw stimulation[13,14]. Previously, Dr. Huang reported and compared time-course expressions of several inflammatory-associated genes in the dorsal root ganglion (DRG) of LPI and SMIR rats, using q-PCR[15]. Besides, their study also applied next-generation RNA sequencing (RNA-seq) to evaluate the time-course transcriptomic variation in the tissue of skin, muscle and DRG, to explore the potential origin of the temporary and persistent postoperative pain, and further to expound pathogenic mechanisms behind the transition of acute to chronic pain. Inspired by the design of previous studies and the technology diffusion of gene sequencing, we implemented this RNA-seq to evaluate the time-course transcriptomic variation in the tissue of skin, muscle and DRG, and further to identify the potential origin and mechanism of CPSP.

Methods

All animal experiments were approved by Animal Care and Use Committee of Navel Medical University, and conformed to the guidelines of the National Institutes of Health Guide for the Care and Use of Laboratory Animals. Male adult (250 to 300 g) Sprague-Dawley rats were housed in a mixed-sex rodent room, and were maintained on a 12-hr light-dark cycle (6am–6 pm) with free available to food and water. Rats were acclimatized to the rodent room for at least 1 week prior to the procedure. A total of 60 rats were used, after baseline mechanical sensitivity measurement, 51 of them were arranged for LPI and SMIR model, 15 were then excluded during the study process. Rats excluded mainly for failure of modeling or local infection. Ultimately 20 rats in SMIR and 16 in LPI group fulfilled the study schedules, with 4 rats were used for tissue collection and RNA-sequencing in each time-point. All rats were sacrificed by euthanasia. The study flow is presented in Fig. 1.

Lateral paw incision. The LPI surgery was performed as previously described. Rats were anesthetized with sevoflurane inhalation anesthetic for quick induction and recovery. A 1-cm longitudinal incision was made along the hairs bordering the lateral plantar surface of the hind paw using scalpel, the depth was through the skin, fascia to the underlying flexor muscle. Pressure applied for a minute to stop bleeding, and the skin was immediately sutured using 5–0 nylon sutures, with topical antibiotics administered. Animals were then separately placed in their own cages for recover. Sutures were removed 36 hours later by when the wound was mostly healed.

Skin/muscle incision and retraction. The SMIR surgery was performed as previously described. Rats were anesthetized with intraperitoneal sodium pentobarbital (CAS:57-33-0, Sigma–Aldrich, St. Louis, MO, USA), at doses of 50 mg/kg. Then rats were lied on their back on operating table. After hair removal and skin sterilization, a 15 mm skin incision was made 5 mm medial to the saphenous vein, to visualize the saphenous nerve and thigh muscle. Then, a short incision, 4 mm medial to the saphenous vein and nerve, was made on the muscle, to allow blunt dissection.

A blunt scissor was used at first to enlarge and deepen the cut, exposing the underlying fascia of the adductor muscles. A customed animal tissue dissecting retractor was then inserted into the full-thickness the of the skin-muscular incision, to retract it by 2 cm and persist for 1 hour. During the retraction, open wound was covered with wet sterile gauze to prevent fluid loss and infection. Animals were transferred to a temperature and closely monitored. After the 1 hour retraction, check for the validity of the skin and muscle. Then skin closure, resuscitation maintained as LPI rats.

Behavioral test. All animals were acclimatized to the behavioral test room for 1 hour before each behavioral test. Animals were placed on an elevated wire mesh surface, mechanical allodynia/ hyperalgesia was detected using Von-Frey monofilaments to the mid-plantar area of the hindpaw encircled by footpads. The filaments with

Sample name†	NCBI SRA DATA Accession	Sample name†	NCBI SRA DATA Accession	Sample name†	NCBI SRA DATA Accession
LPI_0_1_DRG	GSM8278924	LPI_0_1_MUS	GSM8278925	LPI_0_1_SKI	GSM8278926
LPI_0_2_DRG	GSM8278927	LPI_0_2_MUS	GSM8278928	LPI_0_2_SKI	GSM8278929
LPI_0_3_DRG	GSM8278930	LPI_0_3_MUS	GSM8278931	LPI_0_3_SKI	GSM8278932
LPI_0_4_DRG	GSM8278933	LPI_0_4_MUS	GSM8278934	LPI_0_4_SKI	GSM8278935
LPI_1_2_DRG	GSM8278936	LPI_1_2_MUS	GSM8278937	LPI_1_2_SKI	GSM8278938
LPI_1_3_DRG	GSM8278939	LPI_1_3_MUS	GSM8278940	LPI_1_3_SKI	GSM8278941
LPI_1_4_DRG	GSM8278942	LPI_1_4_MUS	GSM8278943	LPI_1_4_SKI	GSM8278944
LPI_1_5_DRG	GSM8278945	LPI_1_5_MUS	GSM8278946	LPI_1_5_SKI	GSM8278947
LPI_2_1_DRG	GSM8278948	LPI_2_1_MUS	GSM8278949	LPI_2_1_SKI	GSM8278950
LPI_2_3_DRG	GSM8278951	LPI_2_3_MUS	GSM8278952	LPI_2_3_SKI	GSM8278953
LPI_2_4_DRG	GSM8278954	LPI_2_4_MUS	GSM8278955	LPI_2_4_SKI	GSM8278956
LPI_2_5_DRG	GSM8278957	LPI_2_5_MUS	GSM8278958	LPI_2_5_SKI	GSM8278959
LPI_10_4_DRG	GSM8278960	LPI_10_4_MUS	GSM8278961	LPI_10_4_SKI	GSM8278962
LPI_10_5_DRG	GSM8278963	LPI_10_5_MUS	GSM8278964	LPI_10_5_SKI	GSM8278965
LPI_10_6_DRG	GSM8278966	LPI_10_6_MUS	GSM8278967	LPI_10_6_SKI	GSM8278968
LPI_10_7_DRG	GSM8278969	LPI_10_7_MUS	GSM8278970	LPI_10_7_SKI	GSM8278971
SMIR_0_1_DRG	GSM8278972	SMIR_0_1_MUS	GSM8278973	SMIR_0_1_SKI	GSM8278974
SMIR_0_2_DRG	GSM8278975	SMIR_0_2_MUS	GSM8278976	SMIR_0_2_SKI	GSM8278977
SMIR_0_3_DRG	GSM8278978	SMIR_0_3_MUS	GSM8278979	SMIR_0_3_SKI	GSM8278980
SMIR_0_4_DRG	GSM8278981	SMIR_0_4_MUS	GSM8278982	SMIR_0_4_SKI	GSM8278983
SMIR_1_1_DRG	GSM8278984	SMIR_1_1_MUS	GSM8278985	SMIR_1_1_SKI	GSM8278986
SMIR_1_2_DRG	GSM8278987	SMIR_1_2_MUS	GSM8278988	SMIR_1_2_SKI	GSM8278989
SMIR_1_3_DRG	GSM8278990	SMIR_1_3_MUS	GSM8278991	SMIR_1_3_SKI	GSM8278992
SMIR_1_4_DRG	GSM8278993	SMIR_1_4_MUS	GSM8278994	SMIR_1_4_SKI	GSM8278995
SMIR_2_1_DRG	GSM8278996	SMIR_2_1_MUS	GSM8278997	SMIR_2_1_SKI	GSM8278998
SMIR_2_3_DRG	GSM8278999	SMIR_2_3_MUS	GSM8279000	SMIR_2_3_SKI	GSM8279001
SMIR_2_4_DRG	GSM8279002	SMIR_2_4_MUS	GSM8279003	SMIR_2_4_SKI	GSM8279004
SMIR_2_6_DRG	GSM8279005	SMIR_2_6_MUS	GSM8279006	SMIR_2_6_SKI	GSM8279007
SMIR_10_3_DRG	GSM8279008	SMIR_10_3_MUS	GSM8279009	SMIR_10_3_SKI	GSM8279010
SMIR_10_4_DRG	GSM8279011	SMIR_10_4_MUS	GSM8279012	SMIR_10_4_SKI	GSM8279013
SMIR_10_5_DRG	GSM8279014	SMIR_10_5_MUS	GSM8279015	SMIR_10_5_SKI	GSM8279016
SMIR_10_6_DRG	GSM8279017	SMIR_10_6_MUS	GSM8279018	SMIR_10_6_SKI	GSM8279019
SMIR_32_1_DRG	GSM8279020	SMIR_32_1_MUS	GSM8279021	SMIR_32_1_SKI	GSM8279022
SMIR_32_3_DRG	GSM8279023	SMIR_32_3_MUS	GSM8279024	SMIR_32_3_SKI	GSM8279025
SMIR_32_4_DRG	GSM8279026	SMIR_32_4_MUS	GSM8279027	SMIR_32_4_SKI	GSM8279028
SMIR_32_5_DRG	GSM8279029	SMIR_32_5_MUS	GSM8279030	SMIR_32_5_SKI	GSM8279031

Table 1. A summary of name scheme and data accession. †The sample naming scheme as: **animal model _ timepoint for tissue harvest _ NO. of the animal _ the sampled tissue**, noting that there have several rats failed for SMIR/LPI modeling, thus, the No. of animal may not be serial numbers.

increasing bending forces of 4 g, 6 g, 10 g and 15 g were applied in order, each filament was applied 10 times, and the number of hindpaw withdrawal was recorded, then the percentage of withdraw response was calculated.

One day prior to the procedures, baseline mechanical sensitivity of all rats was measured, and this time-point was denoted as 0 Day. Rats with abnormal baseline performance were removed. In LPI rats, the mechanical pain was measured at 6 hours, 2 days and 10 days after surgery. While in SMIR, the time points were 6 hours, 2 days, 10 days and 32 days after surgery. The time points were selected according to the previous researches. For rats met the following situations were determined as failure of modeling and removed from the study: significant restriction of movements or disability; local or general infection; delayed wound-healing; unreliable or unexpected allodynia response in each behavioral test. Notably, after the behavioral test and removal in each time-point (including 0 Day), 4 rats in each of the two groups were randomly picked up for tissue harvest.

Skin, muscle and DRG isolation. Rats were deeply anesthetized with isoflurane, transcardially perfused with nuclease-free saline (pH 7.4). The incised skin and muscle tissue were rapidly dissected, the C3-C6 DRGs of LPI and C2-C5 DRGs of SMIR were then extracted. All samples were immediately transferred to ice-cold RNAlater solution (AM7020, Thermo, Waltham, MA, USA) and refrigerated at 4 °C for 48 hours. Then samples were removed from RNAlater solution, placed into fresh 1.5 mL conical tubes and stored at −80°C.

RNA isolation and sequencing. Total RNA was isolated from each thymic sample using the RNAmini kit (52906, Qiagen, Germany). Gel electrophoresis and Qubit (Q33226, Thermo, Waltham, MA, USA) were used to exam the RNA

Sample	RNA_ Concentration (ng/ul)	Average_ length	Raw_reads (Mbp)	Raw_read_ pairs (Mbp)	Raw_bases (Gbp)	Clean.reads (Mbp)	Clean_read_ pairs (Mbp)	Clean_bases (Gbp)	Mapping ratio (%)	Q20 (%)	Q30 (%)	RIN
LPI_ DRG	48.60 (41.201,60.504)	138.72 ± 0.773	36.75 ± 2.015	18.37 ± 1.006	5.55 ± 0.305	34.63 ± 2.223	17.31 ± 1.112	4.8 ± 0.302	95.89 ± 0.2001	98 ± 0.1	94 ± 0.30	8.35 ± 0.516
LPI_ MUS	39.60 (27.655,52.753)	137.44 ± 1.760	37.92 ± 4.520	18.96 ± 2.258	5.73 ± 0.681	35.4 ± 3.696	17.7 ± 1.848	4.86 ± 0.476	96.29 ± 0.280	98 ± 0.1	95 ± 0.2	8.43 ± 0.639
LPI_SKI	358.00 (330.001,449.502)	138.27 ± 1.221	38.66 ± 4.726	19.33 ± 2.364	5.84 ± 0.713	36.49 ± 4.427	18.24 ± 2.214	5.04 ± 0.573	95.75 ± 0.232	98 ± 0.1	95 ± 0.3	8.33 ± 0.626
SMIR_ DRG	23.90 (19.201,28.652)	139.21 ± 1.111	47.33 ± 3.651	23.67 ± 1.825	7.15 ± 0.551	46.12 ± 3.27	23.06 ± 1.634	6.42 ± 0.445	96.44 ± 0.202	98 ± 0.1	94 ± 0.2	8.08 ± 1.046
SMIR_ MUS	190.80 (169.002,220.501)	139.21 ± 1.247	48.80 ± 5.000	24.40 ± 2.500	7.37 ± 0.756	47.59 ± 4.901	23.80 ± 2.450	6.62 ± 0.645	96.67 ± 0.103	98 ± 0.1	94 ± 0.3	8.35 ± 0.350
SMIR_ SKI	199.30 (156.251,240.502)	139.49 ± 0.927	45.94 ± 3.620	22.97 ± 1.811	6.94 ± 0.547	44.47 ± 3.515	22.24 ± 1.758	6.2 ± 0.482	96.08 ± 0.170	98 ± 0.1	94 ± 0.2	8.51 ± 0.443

Table 2. Brief information of RNA quantification, quality control and alignment. RIN: RNA integrity numbers; SKI refers to skin, MUS refers to muscle, DRG refers to dorsal root ganglion. Data are presented as Mean ± SD or Median (interquartile range) accordingly.

Study group	Region	Time Point	Comparison	No. expressed genes	No. DEGs	up-regulated DEGs	down-regulated DEGs
LPI_1_DRG	DRG	6 hours	vs. LPI_0_DRG	22090	286	181	105
LPI_2_DRG	DRG	2 days	vs. LPI_0_DRG	22218	629	525	104
LPI_10_DRG	DRG	10 days	vs. LPI_0_DRG	22184	486	393	93
LPI_1_MUS	muscle	6 hours	vs. LPI_0_MUS	21578	4810	2293	2517
LPI_2_MUS	muscle	2 days	vs. LPI_0_MUS	21891	5502	2601	2901
LPI_10_MUS	muscle	10 days	vs. LPI_0_MUS	21807	994	731	263
LPI_1_SKI	skin	6 hours	vs. LPI_0_SKI	20963	4771	1965	2806
LPI_2_SKI	skin	2 days	vs. LPI_0_SKI	21139	3669	1794	1875
LPI_10_SKI	skin	10 days	vs. LPI_0_SKI	21405	993	869	124
SMIR_1_DRG	DRG	6 hours	vs. SMIR_0_DRG	22727	375	100	275
SMIR_2_DRG	DRG	2 days	vs. SMIR_0_DRG	22782	580	101	479
SMIR_10_DRG	DRG	10 days	vs. SMIR_0_DRG	22804	387	104	283
SMIR_32_DRG	DRG	32 days	vs. SMIR_0_DRG	22829	476	110	366
SMIR_1_MUS	muscle	6 hours	vs. SMIR_0_MUS	20890	4287	2629	1658
SMIR_2_MUS	muscle	2 days	vs. SMIR_0_MUS	21149	6585	3818	2767
SMIR_10_MUS	muscle	10 days	vs. SMIR_0_MUS	21260	6132	3797	2335
SMIR_32_MUS	muscle	32 days	vs. SMIR_0_MUS	20650	1090	814	276
SMIR_1_SKI	skin	6 hours	vs. SMIR_0_SKI	22346	6241	2267	3974
SMIR_2_SKI	skin	2 days	vs. SMIR_0_SKI	22337	4664	1778	2886
SMIR_10_SKI	skin	10 days	vs. SMIR_0_SKI	22484	3006	1492	1514
SMIR_32_SKI	skin	32 days	vs. SMIR_0_SKI	22337	514	327	187

Table 3. A summary of differential expressed genes by study duration, region, and comparison.

quality and RNA integrity number (RIN). All samples had RIN values ≥ 7.0 (Table 2) and at least 10 ng total RNA. For RNA sequencing, RNA samples from four biological replicates at each time point were separated into independent pools, at equal amounts. Strand-specific libraries were constructed using the TruSeq RNA sample preparation kit (RS-122-2001, Illumina, San Diego, CA, USA), and sequencing was carried out by 2 × 150 bp paired-end using the Illumina Novaseq 6000 instrument. The raw data was trimmed by Skewer and the data quality was checked by FastQC (Supplementary Figs. 1–36). Clean reads were aligned to the Rattus norvegicus, genome assembly Rnor_6.0, using STAR. Mapping results were provided in Table 2, with the base ratios of Q20 and Q30 were counted as well. length was.. The expression of the transcript was calculated by FPKM (Fragments Per Kilobase of exon model per Million mapped reads) using Perl. Differentially expression transcripts (DETs) were determined using the MA-plot-based method with Random Sampling (MARS) model in the DEGseq package between different time points (as described in Table 3). Generally, in MARS model, M = log2C1 - log2C2, and A = (log2C1 + log2C2)/2 (C1 and C2 denote the counts of reads mapped to a specific gene obtained from two samples). The thresholds for determining DEGs are $P < 0.05$ and absolute fold change ≥ 2. Numbers of up and down-regulated DEGs in all comparisons presented in Table 3.

Data Records

Complete RNA-seq data were deposited in the NCBI's Gene Expression Omnibus (GEO) database (GSE267799)[16]. The study group, name scheme and data accession information related to each sample are also presented in Table 1 and Supplementary Table S1.

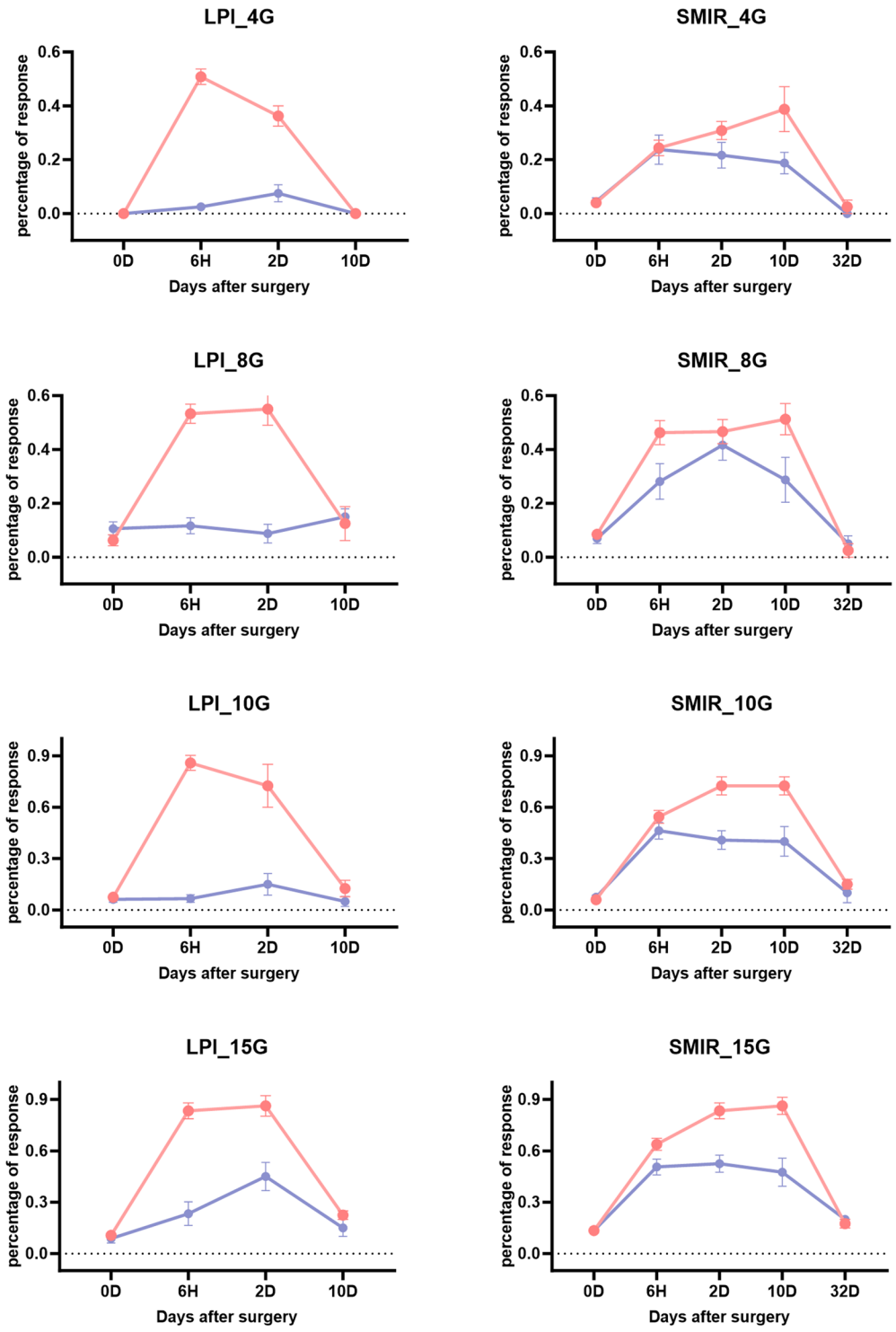

Fig. 2 Mechanical pain assessment of the LPI and SMIR animals sending for sequencing. A total of 108 36 rats were finally used for sequencing, with 16 in LPI while another 20 in SMIR. By each time-point of tissue harvest, the withdrawal threshold of the ipsilateral (red line) and contralateral (blue line) hindpaw of all rats were measured using Von-Frey monofilaments, following an increasing bending forces of 4 g, 6 g, 10 g and 15 g in order.

Technical Validation

All animals had general check-up and behavioral test to verify the pain model, to make sure all samples send for sequencing represented reliable LPI/SMIR animal. The results of mechanical allodynia/hyperalgesia of all rats are exhibited in Fig. 2. Besides, as our samples represent heterogeneous populations of cells in the skin, muscle

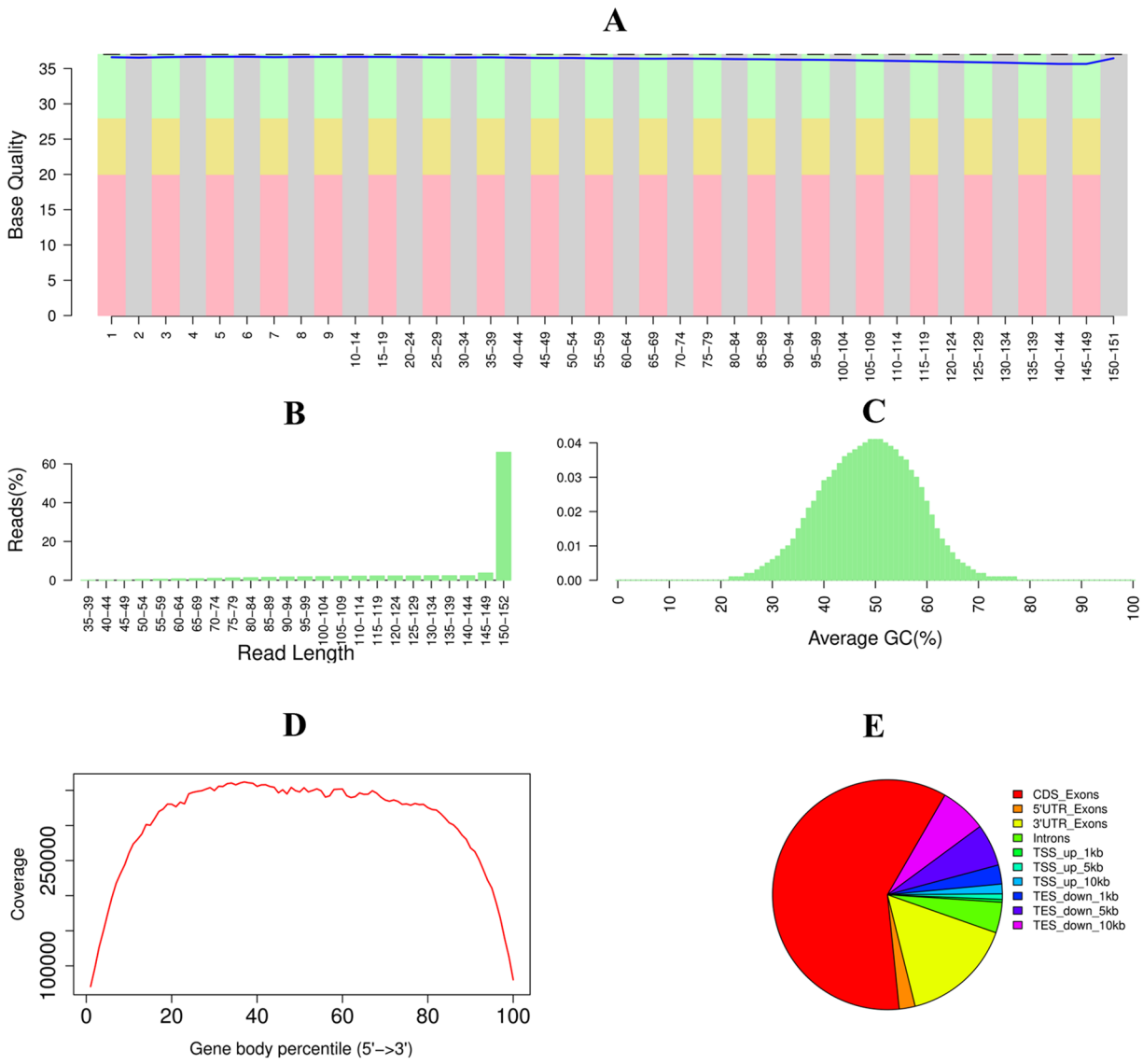

Fig. 3 Representative quality check for RNA-seq. (**A**) Representative quality score distribution for read1 150 bp bases. (**B**) Representative distribution of read1 length. (**C**) Representative distribution of GC content for each read1. (**D**) Regional distribution of all reads mapped to the reference genome. (**E**) Coverage uniformity along with transcripts.

and DRG, the location of incision and extracted tissues were all defined in advance, and all tissues were extracted in certain volume and weight. The name scheme and NCBI data accession of all 108 samples were summarized in Table 1 and more specifically in Supplementary Table S1. The quality of RNA was examined using gel electrophoresis and Qubit. All samples showed clear band in the gel. The measured RNA concentration and RNA integrity numbers (RIN) of all samples were high (Table 2, Supplementary Table S2), which were appropriate for deep sequencing. RNA-seq data quality was determined using FastQC. A representative FastQC report is depicted in Fig. 3. As indicated, the reads had universally high-quality values (Fig. 3A). Meanwhile, the representative distribution of read length showed peak at 150 bp (Fig. 3B), while the distribution of GC content was similar to the theoretical distribution, indicates very low contamination (Fig. 3C). Then, the coverage uniformity along with transcripts was measured, with no significant 5′ or 3′ end bias identified (Fig. 3D). The regional distribution of all reads mapped to the reference genome were also displayed (Fig. 3E). We summarized the general RNA quantification and quality control results of animal models and tissues in Table 2, while the specific sequencing data of each sample were also presented in Supplementary Table S2. The results suggested that the average input fragment size per sample was 150 bp with a mean read depth of 44.36 million, and a high percentage of reads were mapped to the reference rat genome (97.69% alignment; Table 2). Besides, the lowest Q20/Q30 reaches 97.45%/93.50%, which indicates more confident base call (Supplementary Table S2). Table 3 provides summary data of differential expressed genes during the comparisons. PCA plots for the 6 groups are provided in Fig. 4.

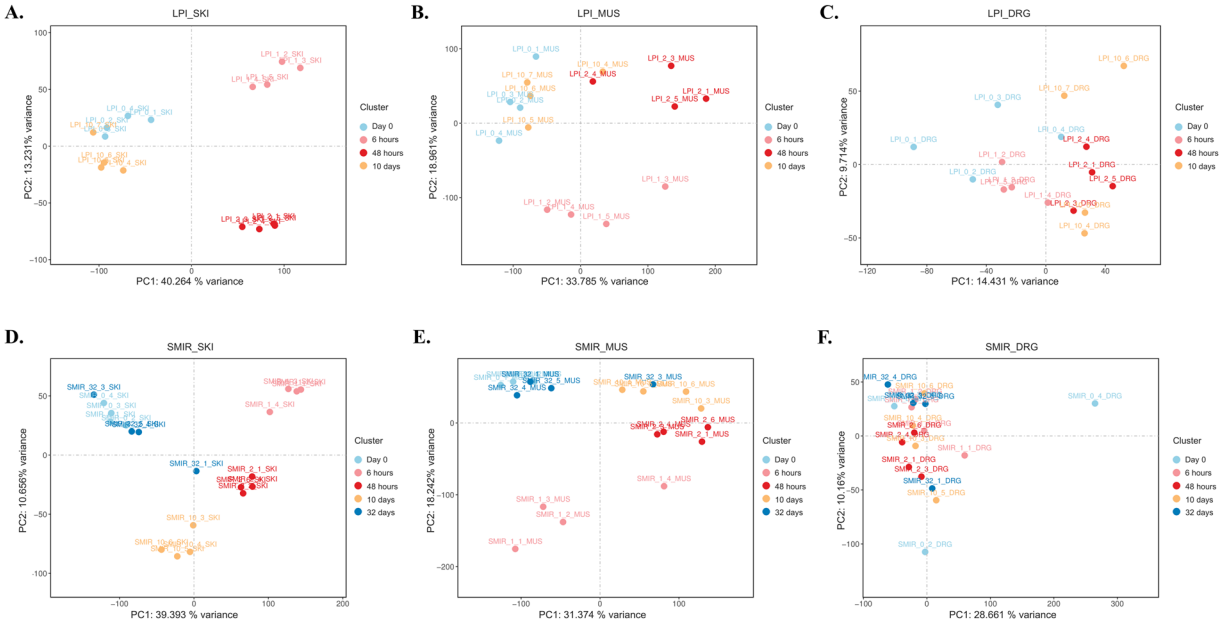

Fig. 4 Principle component analysis (PCA) illustrates the clustering of (**A**) LPI_SKI; (**B**) LPI_MUS; (**C**) LPI_DRG; (**D**) SMIR_SKI; (**E**) SMIR_MUS; (**F**) SMIR_DRG. In each PCA plot, the first two principal components are shown, and the percent of total variation explained by each component is shown in the axis titles. Samples with similar characteristics appear close to each other, and samples with dissimilar characteristics are farther apart.

Code availability

The following open access software was used in this study, and we used default parameters with no custom code was used beyond the tools listed.

1. skewer (version 0.2.2) was used to trim adapters and filter quality read: https://sourceforge.net/projects/skewer/files/?source=navbar.
2. FastQC (version 0.11.5) was used to check the quality of clean reads: http://www.bioinformatics.babraham.ac.uk/projects/fastqc.
3. STAR (version 2.5.2b) was used to map sequence reads to the Rattus Rnor6 genome: https://github.com/alexdobin/STAR.
4. StringTie (version 2.2.1) was used to count the original sequence reads of known genes: http://ccb.jhu.edu/software/stringtie.
5. DESeq2 (version 1.16.1) was used to identify diferentially expressed genes: https://bioconductor.org/packages/release/bioc/html/DESeq2.html.
6. Pheatmap was used to plot the heatmap: https://cran.r-project.org/web/packages/pheatmap/index.html.
7. TopGO was used for GO functional enrichment analysis: http://www.bioconductor.org/packages/release/bioc/html/topGO.html.

Received: 30 May 2024; Accepted: 31 October 2024;
Published online: 14 November 2024

References

1. Glare, P., Aubrey, K. R. & Myles, P. S. Transition from acute to chronic pain after surgery. *Lancet* **393**, 1537–1546, https://doi.org/10.1016/S0140-6736(19)30352-6 (2019).
2. Schug, S. A. *et al.* The IASP classification of chronic pain for ICD-11: chronic postsurgical or posttraumatic pain. *Pain* **160**, 45–52, https://doi.org/10.1097/j.pain.0000000000001413 (2018).
3. Richebé, P., Capdevila, X. & Rivat, C. Persistent Postsurgical Pain: Pathophysiology and Preventative Pharmacologic Considerations. *Anesthesiology* **129**, 590–607, https://doi.org/10.1097/ALN.0000000000002238 (2018).
4. van Driel, M. E. C. *et al.* Development and validation of a multivariable prediction model for early prediction of chronic postsurgical pain in adults: a prospective co hort study. *British journal of anaesthesia* **129**, 407–415, https://doi.org/10.1016/j.bja.2022.04.030 (2022).
5. van Helden, E. V. *et al.* Chronic postsurgical pain after minimally invasive adrenalectomy: prevalence and impact on quality of life. *BMC Anesthesiol* **22**, 153, https://doi.org/10.1186/s12871-022-01696-4 (2022).
6. Buvanendran, A. Chronic postsurgical pain: are we closer to understanding the puzzle? *Anesth Analg* **115**, 231–232, https://doi.org/10.1213/ANE.0b013e318258b9f7 (2012).
7. Kang, Y., Trewern, L., Jackman, J., McCartney, D. & Soni, A. Chronic pain: definitions and diagnosis. *BMJ* **381**, e076036, https://doi.org/10.1136/bmj-2023-076036 (2023).
8. Barroso, J., Branco, P. & Apkarian, A. V. Brain mechanisms of chronic pain: critical role of translational approach. *Transl Res* **238**, 76–89, https://doi.org/10.1016/j.trsl.2021.06.004 (2021).
9. Descalzi, G. *et al.* Epigenetic mechanisms of chronic pain. *Trends Neurosci* **38**, 237–246, https://doi.org/10.1016/j.tins.2015.02.001 (2015).

10. Carley, M. E. *et al*. Pharmacotherapy for the Prevention of Chronic Pain after Surgery in Adults: An Updated Systematic Review and Meta-analysis. *Anesthesiology* **135**, 304–325, https://doi.org/10.1097/ALN.0000000000003837 (2021).
11. Steyaert, A. & Lavand'homme, P. Prevention and Treatment of Chronic Postsurgical Pain: A Narrative Review. *Drugs* **78**, 339–354, https://doi.org/10.1007/s40265-018-0866-x (2018).
12. Antony, A. B. *et al*. Neuromodulation of the Dorsal Root Ganglion for Chronic Postsurgical Pain. *Pain Med* **20**, S41–S46, https://doi.org/10.1093/pm/pnz072 (2019).
13. Flatters, S. J. L. Characterization of a model of persistent postoperative pain evoked by skin/muscle incision and retraction (SMIR). *Pain* **135**, 119–130, https://doi.org/10.1016/j.pain.2007.05.013 (2008).
14. Wang, C.-F., Pancaro, C., Gerner, P. & Strichartz, G. Prolonged suppression of postincisional pain by a slow-release formulation of lidocaine. *Anesthesiology* **114**, 135–149, https://doi.org/10.1097/ALN.0b013e3182001996 (2011).
15. Huang, L., Wang, C.-F., Serhan, C. N. & Strichartz, G. Enduring prevention and transient reduction of postoperative pain by intrathecal resolvin D1. *Pain* **152**, 557–565, https://doi.org/10.1016/j.pain.2010.11.021 (2010).
16. Meng, X., Bu, L., Shen, L. & Tao, K. A transcriptome data set for comparing skin, muscle and DRG between acute and chronic postsurgical pain rats. *Gene Expression Omnibus* https://identifiers.org/geo:GSE267799 (2024).

Acknowledgements

This study was supported by National Natural Science Foundation of China (NO. 82301449), and basic medical research project of Naval Medical University (2022QN095).

Author contributions

Study concept and design: X.Y. Meng, K.M. Tao; drafting of the manuscript: X.Y. Meng; implement the trial: X.Y. Meng; analysis and interpretation of data: X.Y. Meng, L. Bu and L. Shen; revision of the manuscript: K.M. Tao. X.Y. Meng, L. Bu and L. Shen contributed equally to this work, all authors have read and approved the final manuscript.

Competing interests

The authors declare no competing interests.

Additional information

Supplementary information The online version contains supplementary material available at https://doi.org/10.1038/s41597-024-04078-2.

Correspondence and requests for materials should be addressed to K.-m.T.